Materials Chemistry and Physics 131 (2012) 735–742

Contents lists available at SciVerse ScienceDirect

Materials Chemistry and Physics

journal homepage: www.elsevier.com/locate/matchemphys

Carbonization chemistry of heating carbon composites containing novolac/furfuryl alcohol resins and carbon black or mesophase pitch as additives

Xiaoqing Zhang[a,*], Sarah Khor[a], Dachao Gao[a], Elaine Sum[b]

[a] CSIRO Materials Science and Engineering, Private Bag 33, Clayton South, Victoria 3169, Australia
[b] Technology and R&D, Rio Tinto Alcan, Aluval, 725 Rue Aristide Berges, 3834 Voreppe, France

ARTICLE INFO

Article history:
Received 9 May 2011
Received in revised form 27 October 2011
Accepted 30 October 2011

Keywords:
Composite materials
Heat treatment
Polymer
NMR

ABSTRACT

Carbon composites containing novolac/furfuryl alcohol resins with hexamethylene tetramine (HMTA) as a crosslinker and carbon black or mesophase pitch as an additive, were heated to 1000 °C under Argon atmosphere. Carbonization chemistry was studied including the nitrogen-containing structures in the final carbons. The volatiles released during the heating were furfuryl, phenol-benzene species, methane, ethane and other small molecular species such as moisture, CO_2, CO and ammonia. When carbon black was used as an additive in the composite, a considerable amount of furfuryl and phenolic species were "trapped" on the surface of carbon black particles, resulting in a higher carbon yield. Certain carbonization reactions also occurred at lower temperatures, and the dimensional shrinkage was reduced as compared to the resin-only system. On the other hand, the mesophase pitch additive formed homogeneous morphologies with the resin binder, participated in the carbonization process of the resin binder and formed amorphous carbons with porous structures and dimensional expansion. Manipulating the composition and variety of the additives could produce carbon composites with designed performance.

1. Introduction

Phenolic and furfuryl alcohol (FA) resins have been commercially used in various industrial applications [1–7]. Since the resins can form amorphous carbon upon heating to high temperatures with high carbon yield resulting in strong bonding strength to the composites at high temperatures, they have been applied as binders in producing various carbon composites [8–14]. The bonding capability, mechanical properties and processing performance of the carbon composites can be also significantly improved when combining novolac and FA resins as a binder, where the binder viscosity can be controlled by varying the amount of liquid FA in solid novolac resins. Comprehensive studies have been conducted to investigate the curing and carbonization chemistry for phenolic and FA resins [12–27]. The inter-reactions of novolac/HMTA/FA mixing systems were also reported in the literature [28,29] in conjunction with the carbonization behaviour of carbon/phenolic resins composites [30–34]. However, the effect derived from the carbon additives on the carbonization process of the binder phase and the interaction and/or inter-reaction between the binder and additives during the process, which are fundamentally important to the design/modify the performance of carbon composites, have not been investigated in detail.

Leveraging the methodologies and knowledge gained from previous studies, we have conducted research on carbon composites using novolac/HMTA/FA resins as the binder with carbon black or mesophase pitch as additives to modify the mechanical and binding/processing performance for producing advanced carbon materials. Following the report of crosslinking chemistry of curing these systems [35], carbonization of the carbon composites up to 1000 °C were examined and are reported in this paper including the chemical nature of volatiles released during heating, reaction pathways, chemical structures formed during the process, and the morphologies of the final carbon composites. The effects derived from carbon black or mesophase additives on the carbonization chemistry and the final structures of the carbon materials are also discussed.

2. Experimental

2.1. Raw materials and sample preparation

The details of the raw materials used have been reported previously [35]. Novolac resin (Resinox GC 1848), hexamethylene tetramine (HMTA) and furfuryl alcohol (FA: UCAR C34) were obtained from Huntsman Chemical Australia, Merck Pty Ltd and Orica Australia respectively. Carbon black and mesophase pitch (AR

* Corresponding author. Tel.: +61 3 95452653; fax: +61 3 95441128.
E-mail address: Xiaoqing.Zhang@csiro.au (X. Zhang).

0254-0584/$ – see front matter © 2011 Elsevier B.V. All rights reserved.
doi:10.1016/j.matchemphys.2011.10.044

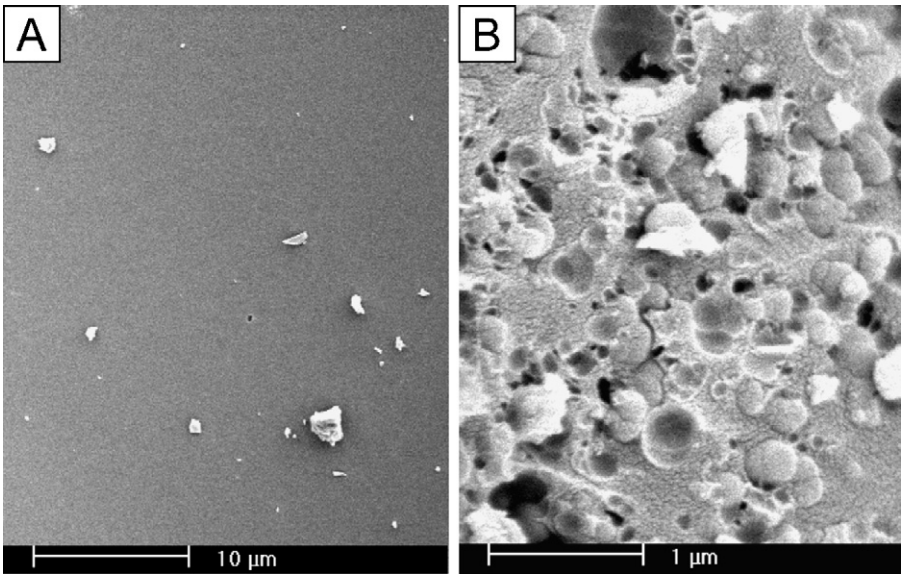

Fig. 1. SEM images of the fracture surfaces of NHF-R (A) and NHF-C (B) after heating to 1000 °C.

Resin MP-P) were supplied by CanCarb Ltd. Canada and Mitsubishi Gas Chemical Company Inc. All raw materials were used as received without purification or any further treatment.

The procedure of green composite preparation was also the same as reported previously [35]. Solid novolac and HMTA were dissolved in FA liquid under mechanical stirring at a speed of 1050 rpm over 3 h to achieve a homogenous system (NHF-R:Novolac:HMTA:FA = 24:5:34 in weight parts). Carbon black or mesophase pitch was then mixed with the resin (resin:additives = 63:37 in weight parts) using a high speed mixer at 3000 rpm for 3–4 min to produce NHF-C or NHF-M green composite sample with additives homogeneously dispersed in the binder. After curing these samples on a small scale (5–8 g) following a slow curing cycle up to 205 °C [35], the cured samples (in cylindrical shape with diameter of ~10 mm) were cooled down to room temperature naturally and taken from the glass vials. Further heat-treatment was conducted using a home-made furnace under Argon atmosphere at a rate of 50 °C h^{-1} from room temperature to a target temperature between 300 and 1000 °C, and finally held at 1000 °C for 2 h. The weight loss values of the samples collected at different temperatures were measured after cooling the samples to room temperature. The diameters of these cylindrical samples were also measured before and after heating to each target temperature and the sample dimensional shrinkage or expansion was determined based on the diameter change.

2.2. Characterization techniques

The fracture surfaces of the composite samples were examined by scanning electron microscopy (SEM) using a Philips FEI XL-30 SFEG instrument. The samples were sputter coated with gold of 20 nm thickness under argon atmosphere. The electron beam with an accelerating voltage of 5 kV was used to produce high definition images.

Elemental analysis of the baked samples was conducted by Chemical & Micro Analytical Service Pty. Ltd. (CMAS, Belmont VIC 3216 Australia).

The X-ray diffraction (XRD) experiment was conducted using a Siemens D5000 XRD with copper radiation at 40 kV and 30 mA over a 2θ range of 10–40° with a 0.03° step and a 4 s step time. A graphite monochromator was used in the diffracted beam.

Thermogravimetric analysis Fourier transform infrared spectroscopy (TGA-FTIR) results were acquired using a TA SDT Q Series Explorer (Q600) TGA connected to a Nicolet Nexus 670 IR Spectrometer in an inert atmosphere (nitrogen gas). A small amount of each pre-cured sample was ground into find powder, placed in the TGA sample pan (~30 mg) and heated following an accelerated rate (500 °C h^{-1}) to 1000 °C then held isothermally for 5 min. Volatiles generated from heating samples in the TGA furnace were transferred through an interface into the FTIR spectrometer maintained at 180 °C. IR spectra were acquired continuously with KBr Beam splitter, resolution of 4 cm^{-1} and 365 scans for each spectrum.

As reported previously [35], $^{13}C/^{15}N$ 97–98% enriched HMTA was used instead of conventional HMTA to prepare the samples for high-resolution solid-state nuclear magnetic resonance (NMR) experiments in order to enhance the signals derived from HMTA. All NMR measurements were conducted at room temperatures using a Varian Unity plus-300 spectrometer at resonance frequencies of 75 MHz for carbon-13 and 30 MHz for nitrogen-15 under conditions of cross polarization (CP), magic angle sample spinning (MAS) and high-power dipolar decoupling (DD) as described previously [35]. The 90° pulse-width was of 5.8 μs while the contact time was 3 ms. The rate of MAS was at a value around 7–8 kHz and no spinning side band was observed for ^{15}N spectra when using such a MAS rate. The chemical shift of ^{13}C spectra was determined by taking the adamantine peak at upfield (29.5 ppm relative to TMS) as an external reference. For ^{15}N spectra, the enriched HMTA resonance at 44 ppm was taken as an external reference.

3. Results and discussion

3.1. Morphology of the carbon composites

Heating NHF-R and NHF-C to 1000 °C resulted in formation of carbon materials with fracture surfaces shown in Fig. 1. A homogeneous morphology was obtained for NHF-R containing a minimal number of pores with pore size less than 1 μm (Fig. 1A). The SEM image of the NHF-C sample after heating to 1000 °C shows that carbon black particles were homogeneously distributed in the binder phase and the pore size was also less than 1 μm (Fig. 1B). Porous morphology was obtained for the NHF-M sample during heating (Fig. 2A–E) and the pore size was varied over a broad range of

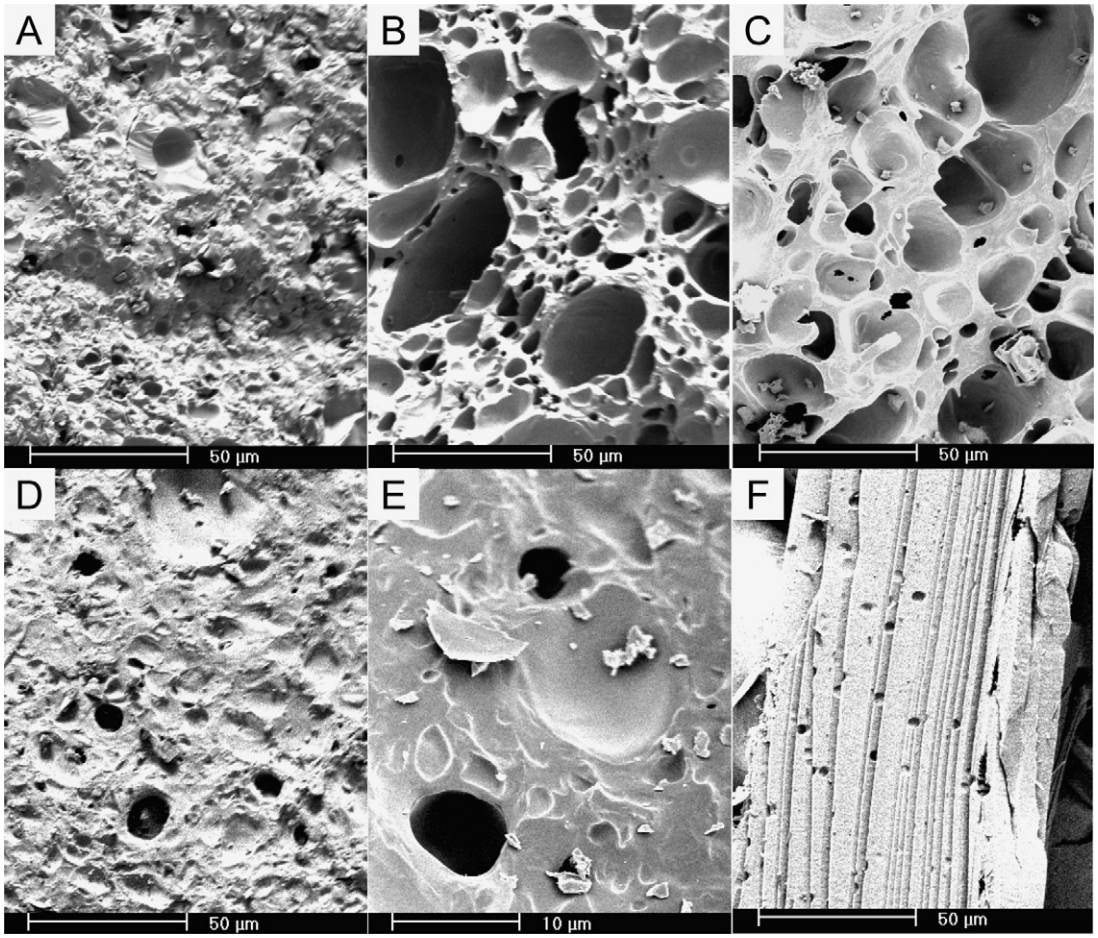

Fig. 2. SEM images of the fracture surfaces of NHF-M after heating to 300 °C (A), 400 °C (B), 600 °C (C) and 1000 °C (D and E), and mesophase-pitch alone after heating to 900 °C (F).

5–50 μm. Large pore size was most prominent when the sample was heated to 400–600 °C. However, the mesophase pitch in the NHF-M system did not form fibrous carbon as it did when heated alone (Fig. 2F). Although the mesophase pitch and the binder resins could have formed crosslinked networks through the whole material with homogeneous morphologies at small scales during the curing process [35], the porous carbon morphology of the NHF-M system was different from those of NHF-R or mesophase-pitch alone samples.

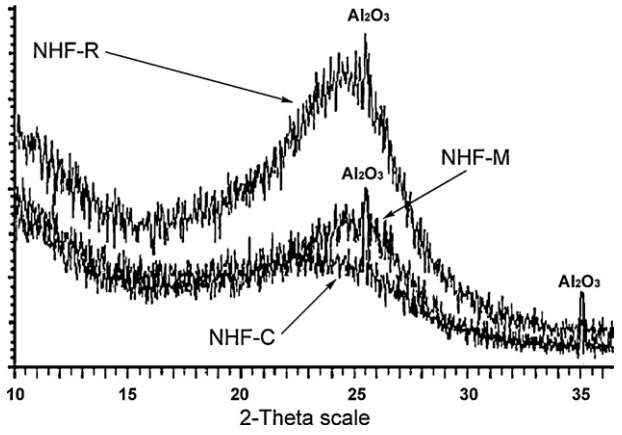

Fig. 3. XRD patterns of NHF-R, NHF-C and NHF-M samples after heating to 1000 °C.

The broad XRD curves shown in Fig. 3 indicated that heating NHF-R, -C and -M to 1000 °C resulted in amorphous carbons. The graphitic crystallinity was minimal even for the NHF-M system where a graphitic structure could be formed when heating mesophase pitch alone. The sharp peaks in the patterns were due to Al_2O_3 impurities, derived from the Al_2O_3 sample-holder during heating.

The weight loss and sample dimensional changes (shrinking or expanding) of NHF-R, -C and -M samples during the heating process are shown in Fig. 4, with the weight loss data in curing up to 205 °C [35] also included. The major proportion of the weight loss (volatile release) occurred below 700 °C. NHF-R released the highest amount of volatiles during the heating, followed by NHF-M, and then NHF-C. The total weight loss for NHF-R was 57%, while that of NHF-C was 30%, which is relatively lower (should be ~37% if assuming no weight loss contribution from carbon black). Although carbonization of mesophase pitch also generated weight loss [9,31,34], the value was lower than that from heating NHF-R resins. Overall, 47% weight loss was detected for heating the NHF-M sample.

Both NHF-R and -C samples experienced a dimensional shrinkage during the heating. The additional micro-pore structures (Fig. 1B) generated in the system compensated the shrinkage of NHF-C to some extent, thus the shrinkage value (~10%) was lower than that of NHF-R (~23%).

In contrast, a dimensional expansion occurred to NHF-M during heating and a maximum expansion was reached at ~500 °C (Fig. 4) due to formation of porous structures with large pore sizes as shown in Fig. 2B and C. The molecular structures of aromatic

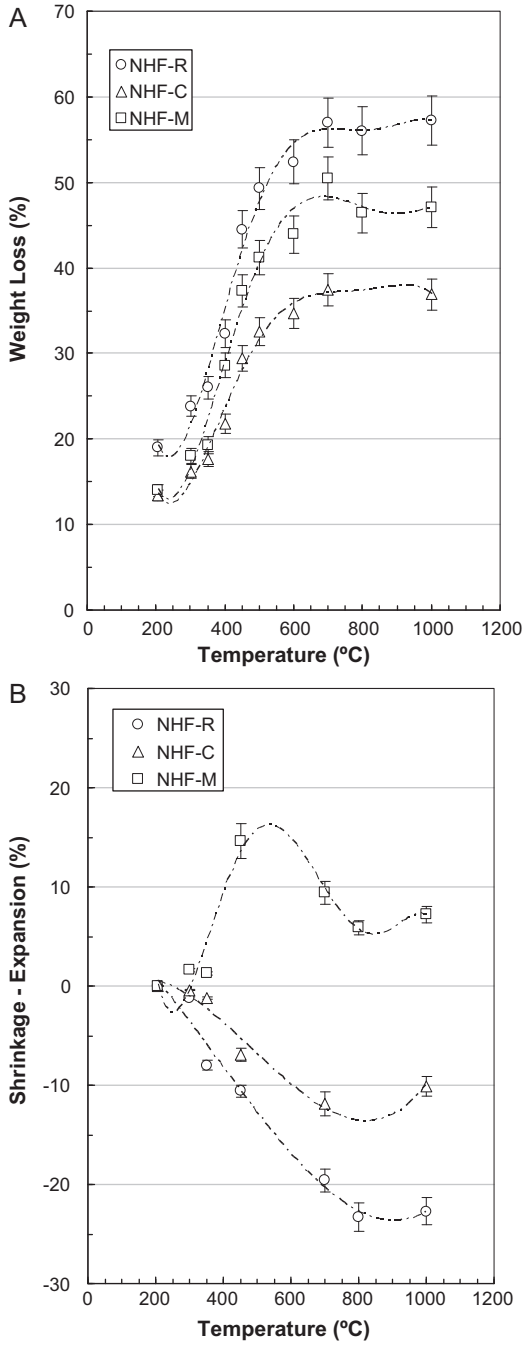

Fig. 4. Weight loss (A) and sample dimensional extension (B) for NHF-R, NHF-C and NHF-M after heating to 1000 °C.

mesophase pitch were similar, volatile release due to carbonization reactions all occurred within a small temperature range, producing significantly porous structures and severe dimensional expansion [31,34,36]. The pore size decreased after heating to above 500 °C possibly due to a certain increase in chain mobility at high temperatures. The final sample expansion for NHF-M up to 1000 °C/2 h was 6–7%.

3.2. Chemical nature of the volatiles released during heating

The large weight loss reflects a significant amount of volatiles released during the heating process. TGA-FTIR was used to study the evolution and chemical nature of these volatiles, where powder samples and a faster heating rate (500 °C h^{-1}, 10 times faster than that in furnace baking) were used to enhance the volatile signals detected in the measurement. The weight loss data detected by the TGA are listed in Table 1. Although these data are lower than those in furnace heating, the trend was similar.

Table 1
Weight loss data (wt%) after heating to 1000 °C.

Samples	NHF-R (%)	NHF-C (%)	NHF-M (%)
Furnace heating	57.2	36.9	47.1
TGA	49.2	30.3	42.4

FTIR spectra of the volatiles released from heating NHF-R in TGA to various temperatures are shown in Fig. 5. These FTIR spectra were compared with standard library spectra available in the spectrometer software, thus the chemical nature of the major products was determined as shown in Fig. 5. At 200 °C, water and furfuryl compounds (FUR) were the predominant volatiles released from the system. CO_2, CO and NH_3 were also generated at increased temperatures in conjunction with CH_4, C_2H_6 and their low molecular weight homologues plus benzene products. Note that above 600 °C, most of these volatile species were still present, and the small molecular species (CO_2, CO, NH_3 and water) could be detected until 1000 °C.

The results of NHF-C and -M were similar to those observed for the NHF-R system but different volatile species displayed different relative intensities. Fig. 6 shows the relative IR intensities of the volatiles released at different temperatures for the three different systems. For NHF-R, release of FUR reached a maximum at 300 °C, but the signal was always detected up to 1000 °C. CO_2 and CO components reached their maximum intensities at 460 °C. Benzene/phenol species and CH_4, C_2H_6 were observed above 400 °C and reached their maximum intensities at 560 °C. Water vapor was released from the system across a broad temperature range although the relative intensity was low, while NH_3 displayed two maximum peaks at 500 and 770 °C.

For NHF-C, CO_2, CO, CH_4, NH_3 and water vapor released similarly as those of NHF-R, but the relative intensities of FUR and phenolic components in the volatiles were significantly decreased. These species could be potentially "trapped" on the surface of carbon black particles, and took part in the carbonization reactions and eventually became part of carbon structures rather than being released as volatiles. The result is consistent with the high carbon yield for the NHF-C sample. For the NHF-M sample, the relative intensities of most volatile components were higher than those in NHF-R and -C systems, but the intensity of CO_2 was relatively lower. On the other hand, CO_2 and CO reached their maximum intensities at higher temperatures, while the maximum intensities of FUR/Ph and CH_4/C_2H_6 species were reached at lower temperatures as compared to those in NHF-R and -C systems. These results could be attributed to the porous structures of the NHF-M system.

The usage of powdered samples in the TGA-FTIR experiment in conjunction with a fast heating rate, reduced the likelihood of volatiles to participate in further reactions during heating, thus the carbon yield would be lower. Composites manufacturing under industrial scale heating processes would have a much smaller material surface area to volume ratio and a longer volatile escape pathway, which would result in benzene/phenol molecules taking part in further polymerization and thermal crosslinking and finally retained in the carbon composites. Therefore, the results from current TGA-FTIR experiment are only indicative for the species which would most likely to form and be released as volatiles during the heating process.

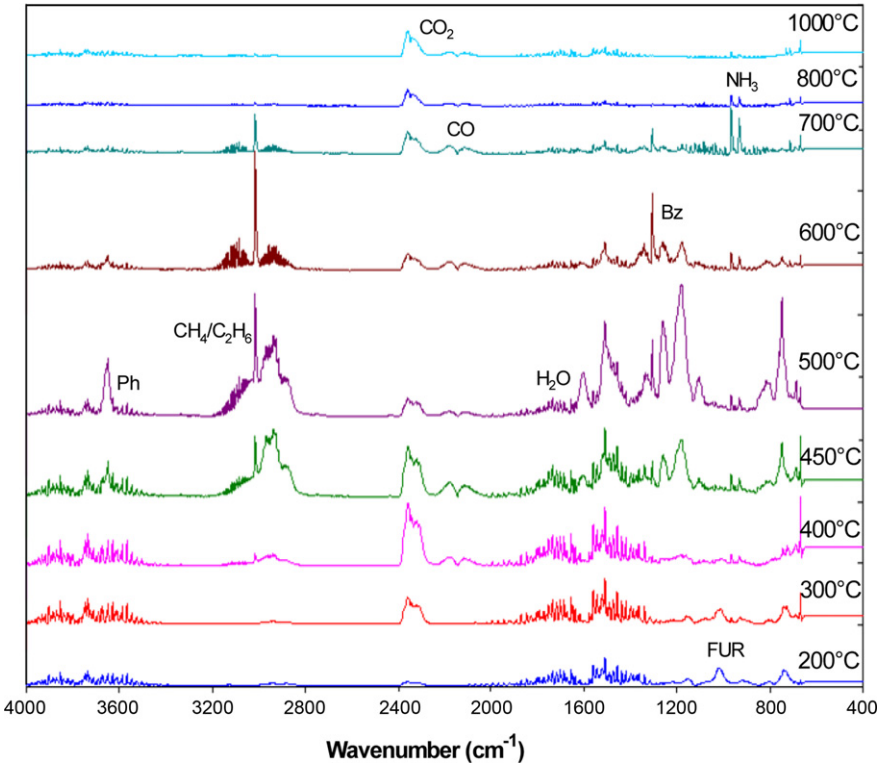

Fig. 5. FT-IR spectra of the volatiles released from NHF-R during TGA up to 1000 °C.

3.3. *Carbonization chemistry of the carbon composites*

The carbon/hydrogen (C/H) atomic ratio is another important parameter (reflecting aromaticity of carbons) in characterizing the carbon composites. The C/H ratio of the carbon black sample used in this study was 20.3, providing an indication of the aromaticity of amorphous carbons. The C/H ratio for the mesophase pitch before heating was 1.57, slightly higher than that of NHF-R sample after curing to 205 °C/4 h (~1.1). The changes of C/H ratio of NHF-R, -C and -M systems during heating are shown in Fig. 7A. Significant increase in the C/H ratio occurred above 600 °C for all the systems, and NHF-C reached a C/H ratio of 12.5 at 1000 °C due to the contribution of carbon black, while the C/H ratios of NHF-R and -M reached 9 and 10 at 1000 °C, respectively. The similar carbonization behaviour of NHF-R and -M systems could be attributed to the strong interactions even chemical linkages between the binder and the additives in the cured sample [35], thus the mesophase pitch could not follow its own graphitization pathway in the carbonization process. Therefore, amorphous carbon was obtained for the NHF-M system.

Fig. 7B shows the nitrogen-content (N%) values of the three systems after heating. The increase in N% in NHF-R at 400–600 °C was due to a larger weight loss of non-nitrogen-containing products as seen in the TGA-FTIR study. The release of nitrogen-containing structures (e.g. NH_3) occurred mainly above 600 °C. A similar behaviour was observed in NHF-C and -M samples, although not that significantly. After heating to 1000 °C, the nitrogen retention for the NHF-R, -C and -M systems were 35.4%, 35.3% and 39.9%, respectively. As the absolute N% content was very low in NHF-C and -M systems, and the difference among these systems was within the measurement error. The chemical structures formed in the solid phase of these composite systems during the heating process were examined by high-resolution solid-state NMR spectroscopy. ^{13}C CP/MAS spectra of NHF-R, -C and -M samples after heating to different temperatures are shown in Fig. 8. The signals derived from HMTA were greatly enhanced due to the use of $^{13}C/^{15}N$ enriched HMTA. A strongly enhanced peak at 103 ppm was detected for NHF-R at 300 °C, and its intensity further increased when the temperature reached 400 °C. The resonances were assigned to >CH═CH< species which were derived from thermal dehydrogenation of methylene linkages (originally from HMTA) during heating. An increase in the methyl group intensity at 15–20 ppm was also observed at increased temperatures. Above 500 °C, a broad peak at 126 ppm was dominant as attributed to the formation of benzene structures while the methylene intensity was even lower than that of methyl groups. The intensities of methylene and methyl resonances became minimal when NHF-R was heated to 600–800 °C. These results were consistent with those reported previously [29]. After heating to 1000 °C, a broad peak was detected due to the formation of amorphous carbon materials.

Both solid-state NMR and TGA-FTIR studies indicate that the major carbonization reactions of NHF-R occurred at 300–600 °C with the opening of furan rings and then the aliphatic structures converting to aromatic benzene structures. Dehydrogenation of the methylene linkages during the heating resulted in formation of >CH═CH< species, then converting to benzene structures and finally producing carbon materials with increased C/H ratio. Methyl groups were also formed during the process and most of them were thermally decomposed from the network and released as CH_4 or C_2H_6, as detected by the TGA-FTIR.

The ^{13}C NMR spectra of the NHF-M samples were similar to those of NHF-R. However, the ^{13}C resonances of the NHF-C samples became broader, suggesting a broad distribution of chemical structures and motional modification of the binder segments due to the strong interactions between the binder and carbon black particles. The carbonization reactions also shifted to lower temperatures; the spectrum at 400 °C for NHF-C was similar to that at 500 °C for NHF-R or NHF-M, indicating dehydrogenation of methylenes occurred at

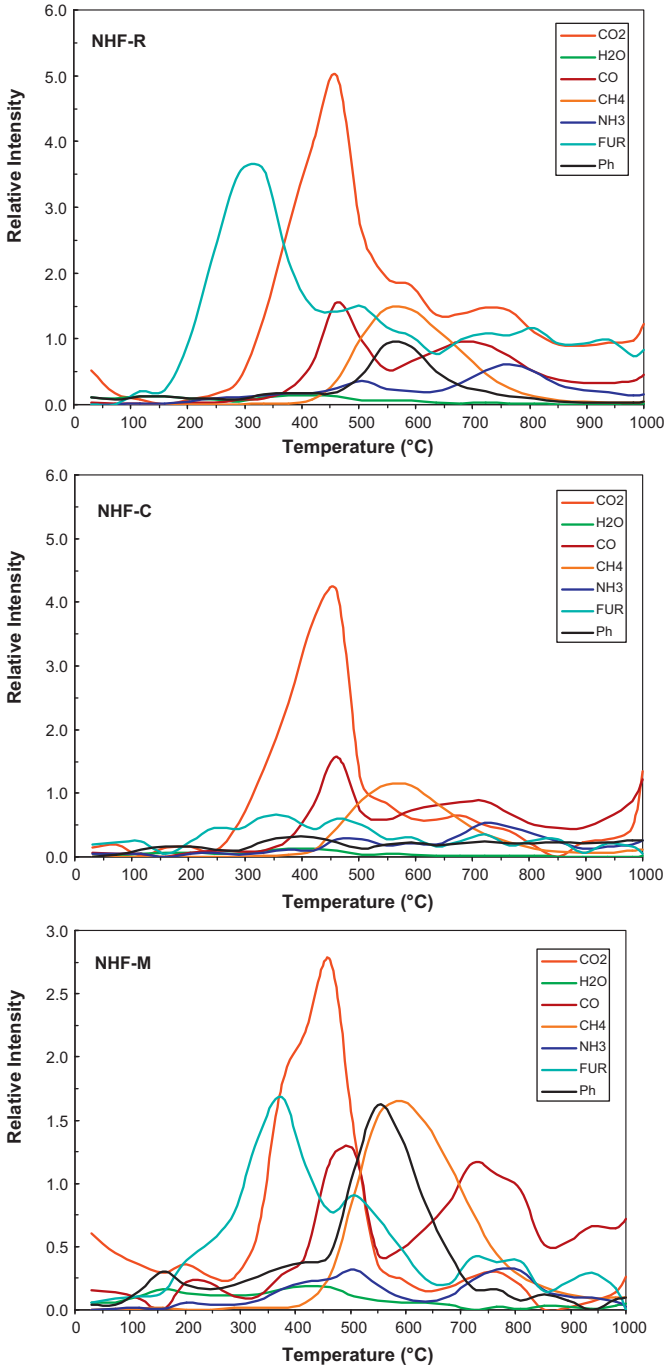

Fig. 6. FT-IR relative intensities of the volatiles released during TGA for NHF-R, NHF-C and NHF-M up to 1000 °C.

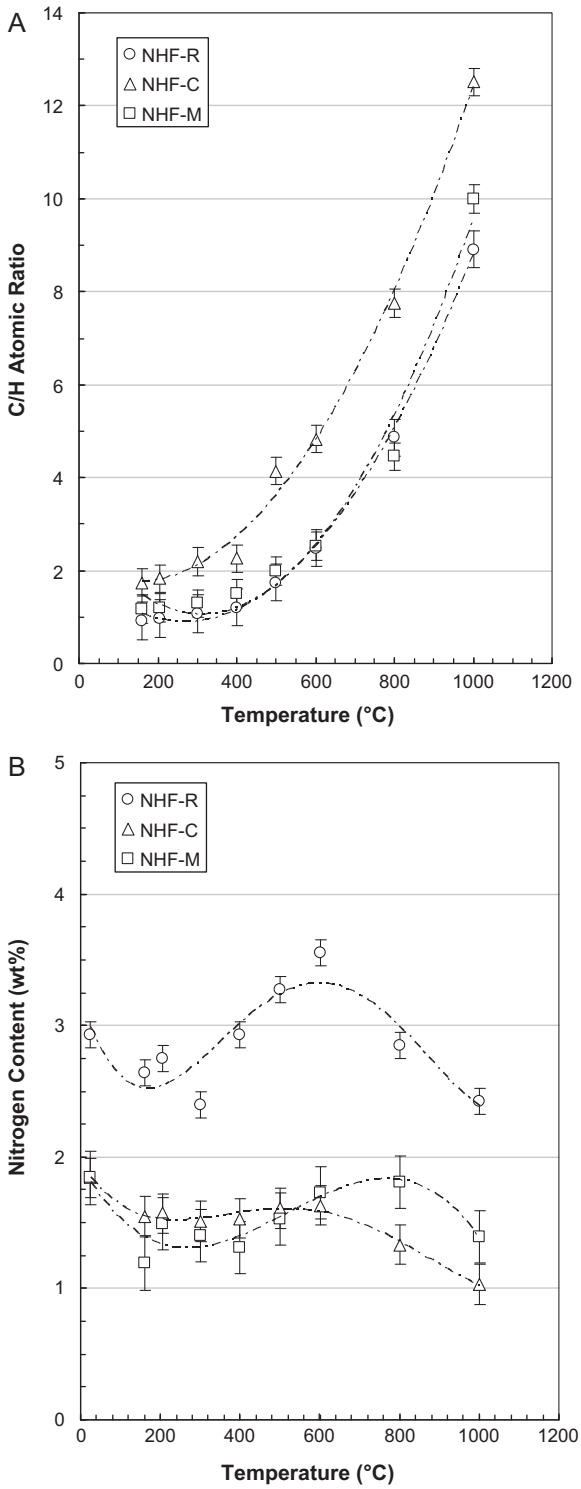

Fig. 7. Atomic C/H ratio (A) and nitrogen content data (B) for NHF-R, NHF-C and NHF-M samples after heating to 1000 °C.

lower temperatures in NHF-C system. These results provide further evidence to explain the lower amount of FUR/Ph volatile release and higher carbon yield for the NHR-C system.

The nitrogen-containing structures of NHF-R and -M samples were examined by ^{15}N CP/MAS spectra and are shown in Fig. 9. The major nitrogen-containing structures in NHF-R after heating to 300 °C were amides and imides (120–150 ppm). Small amounts of nitriles (~250 ppm) and imines (280–320 ppm) were also detected. Increasing temperature produced broad imides/amides peaks and the relative intensity of imines at 280 ppm was further increased after heating to 500–600 °C. NO_2 species were also detected at 450 ppm with the disappearance of the amides/imides resonances when NHF-R was heated to 800 °C. Since the heat-treatment was conducted under argon atmosphere, the oxygen necessary for the oxidation could only come from the decomposition of the phenolic-furfuryl structures. The minor peaks at 30–60 ppm were due to amine species formed by thermal decomposition of the nitrogen-containing linkages of the network. After heating to 800 °C, mainly three broad peaks were detected at 150, 300 and 450 ppm corresponding to residual imides, nitriles and –NO_2 species, respectively.

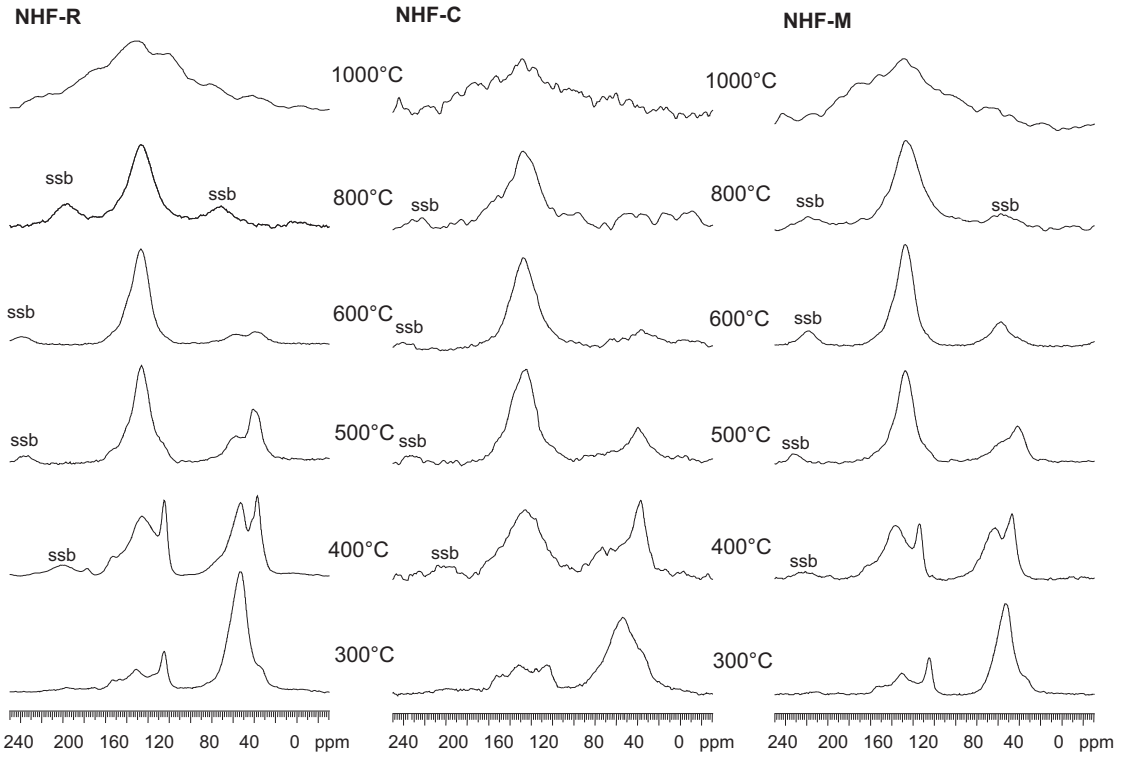

Fig. 8. ^{13}C CP/MAS NMR spectra for NHF-R, NHF-C and NHF-M samples after heating to 1000 °C.

These nitrogen-containing structures acted as impurities in the carbon materials, and could only exist either as linkages between large pieces of carbon structures or at the edge of carbon structures.

Heating the NHF-M system generated similar nitrogen-containing structures as those in NHF-R (Fig. 9), but the relative intensities of imine and nitrile structures were relatively lower in the NHF-M system while the imide structure became the major nitrogen-containing structure remaining until 600 °C. For NHF-C, the ^{15}N signal was very weak and broad (not shown here), possibly due to strong interactions between resin segments and carbon black particles.

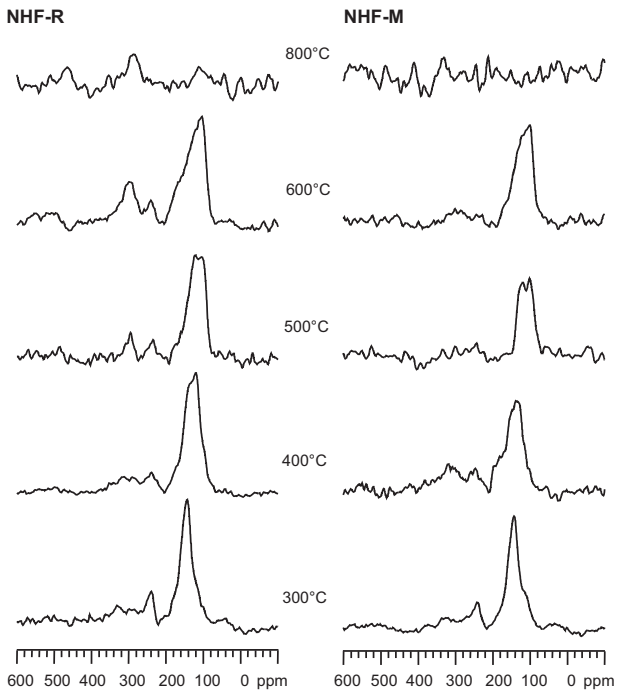

Fig. 9. ^{15}N CP/MAS NMR spectra for NHF-R and NHF-M samples after heating to 800 °C.

These results indicate that carbon black and mesophase pitch additives displayed different behaviour in the composite carbonization process. Application of both additives and manipulating their compositions with the resin binder might be able to provide complementary benefits in carbon composite. In addition, the existence of different amounts and varied nitrogen-containing structures would influence many properties of the carbon materials, e.g. conductivity, wetting performance of liquids or melt substance on the surface of the carbon, or even the mechanical performance. Further research will be conducted to correlate the composite properties with the carbon structures, and determine optimum carbonization conditions of the mixing systems to produce carbon composites with designed performance.

4. Conclusion

Heating the carbon composites (containing novolac/furfuryl alcohol resins as a binder and carbon black or mesophase pitch as additives) to 1000 °C generated amorphous carbons with nitrogen-containing structures. The volatiles released during the process were furfuryl compounds, phenol–benzene species, methane, ethane and other small molecules such as water vapor, CO_2, CO and ammonia. Carbon black and mesophase pitch additives displayed different effects on the carbonization process and the morphologies of the final carbons. Carbon black was homogeneously distributed in the binder phase. The “trapped” resin segments on the surface of carbon black particles took part in the further carbonization, therefore, the carbon yield was increased and the amount of furfuryl/phenolic volatile release was decreased during the heating process. The distribution of chemical structures of the binder segments became broad and their molecular motions were also

modified. Certain carbonization reactions were also shifted to lower temperatures in the system with carbon black as an additive. On the other hand, the mesophase pitch additive participated in the carbonization process of the resin binder and formed amorphous carbons with porous structures and dimensional expansion. A carbon material with complementary performance could be produced by using both carbon black and mesophase additives through manipulating their compositions with resin binders under optimum carbonization conditions.

Acknowledgements

The authors are grateful to Dr Shiqin Yan, Ms Jennifer Peck and Mr Robert Simmonds for their contribution in sample preparation and project discussion, and funding support from Rio Tinto Alcan.

References

[1] R.W. Martin, Chemistry of Phenolic Resins, Wiley, New York, 1956.
[2] A.P. Dunlop, F.N. Peters, The Furans, Reinhold, New York, 1953.
[3] N.J.L. Megson, Phenolic Resin Chemistry, Butterworths, London, 1958.
[4] A. Knop, W. Scheib, Chemistry and Application of Phenolic Resins, Springer-Verlag, 1979.
[5] A. Knop, L. Pilato, Phenolic Resins, Springer-Verlag, New York, 1979.
[6] A. Knop., L. Pilato, Phenolic Resins: Chemistry, Applications and Performance: Future Directions, Springer-Verlag, Berlin, 1985.
[7] L. Pilato, Phenolic Resins: A Century of Progress, Springer-Verlag, Berlin/Heidelberg, 2010.
[8] K. Kanno, J.J. Fernandez, F. Fortin, Y. Korai, I. Mochida, Carbon 35 (1997) 1627.
[9] K. Kanno, N. Koike, Y. Korai, I. Mochida, M. Komatsu, Carbon 37 (1999) 195.
[10] N. Cunningham, M. Lefèvre, J.P. Dodelet, Y. Thomas, S. Pettelier, Carbon 43 (2005) 3054.
[11] M. Yoonessi, H. Toghiani, R. Wheeler, L. Porcar, S. Kline, C.U. Pittman, Carbon 46 (2008) 577.
[12] B. Amram, F. Laval, J. Appl. Polym. Sci. 37 (1989) 1.
[13] C.A. Fyfe, A. Rudin, W. Tchir, Macromolecules 13 (1980) 1320.
[14] S.A. Sojka, R.A. Wolfe, G.D. Guenther, Macromolecules 14 (1981) 1539.
[15] G.E. Maciel, I.S. Chuang, G.E. Myers, Macromolecules 15 (1982) 1218.
[16] C.A. Fyfe, M.S. McKinnon, A. Rudin, W.J. Tchir, Macromolecules 16 (1983) 1216.
[17] R.L. Bryson, G.R. Hatfield, T.A. Early, A.P. Palmer, G.E. Maciel, Macromolecules 16 (1983) 1669.
[18] G.R. Hatfield, G.E. Maciel, Macromolecules 20 (1987) 608.
[19] A. Gupta, I.R. Harrison, Carbon 32 (1994) 953.
[20] S. Glowinkowski, Z. Pajak, Carbon 20 (1982) 13.
[21] A. Shindo, K. Izumino, Carbon 32 (1994) 1233.
[22] Z. Wang, Z. Lu, X. Huang, R. Xue, L. Chen, Carbon 36 (1998) 51.
[23] X. Zhang, M.G. Looney, D.H. Solomon, A.K. Whittaker, Polymer 38 (1997) 5835.
[24] X. Zhang, D.H. Solomon, J. Polym. Sci. B: Polym. Phys. 35 (1997) 2233.
[25] X. Zhang, D.H. Solomon, Polymer 39 (1998) 6153.
[26] A.S.C. Lim, D.H. Solomon, X. Zhang, J. Polym. Sci. A: Polym. Chem. 37 (1999) 1347.
[27] K. Lenghaus, G.G. Qiao, D.H. Solomon, C. Gomez, F. Rodriguez-Reinoso, A. Sepulveda-scribano, Carbon 40 (2002) 743.
[28] X. Zhang, D.H. Solomon, Chem. Mater. 10 (1998) 1833.
[29] X. Zhang, D.H. Solomon, Chem. Mater. 11 (1999) 384.
[30] K.A. Trick, T.E. Saliba, Mechanisms of the pyrolysis of phenolic resin in a carbon/phenolic composite, Carbon 33 (1995) 1509–1515.
[31] K. Kanno, N. Koike, Y. Korai, I. Mochida, Carbon 36 (1998) 869.
[32] K.A. Trick, T.E. Saliba, S.S. Sandhu, Carbon 35 (1997) 393.
[33] I. Mochida, Y. Korai, C.H. Ku, F. Watanabe, Y. Sakai, Carbon 38 (2000) 305.
[34] M. Dumont, M.A. Dourges, X. Bourrat, R. Pailler, R. Naslain, O. Babot, M. Birot, J.P. Pillot, Carbon 43 (2005) 2277.
[35] X. Zhang, S. Khor, D. Gao, E. Sum, Mater. Chem. Phys. 129 (2011) 228.
[36] K. Murakami, M. Okumura, M. Yamamoto, Y. Sanada, Carbon 34 (1996) 187.